Evidence for Two Types of Low-Energy Charge Transfer Excitations in Sr_2CuO_3

A. S. Moskvin,[1] J. Málek,[2,3] M. Knupfer,[2] R. Neudert,[2,*] J. Fink,[2] R. Hayn,[4,2] S.-L. Drechsler,[2,†] N. Motoyama,[5] H. Eisaki,[5,6] and S. Uchida[5]

[1]*Ural State University, 620083 Ekaterinburg, Russia*
[2]*Leibniz-Institut für Festkörper- und Werkstoffforschung Dresden, P.O. Box 270116, D-01171 Dresden, Germany*
[3]*Institute of Physics, ASCR, Na Slovance 2, CZ-18221 Praha 8, Czech Republic*
[4]*Laboratoire Matériaux et Microélectronique de Provence, 13384 Marseille Cedex 13, France*
[5]*Department of Superconductivity, The University of Tokyo, Bunkuyo-ku, Tokyo 113, Japan*
[6]*Nanoelectronic Research Institute, National Institute of Advanced Industrial Science and Technology, Tsukuba, 305-8568, Japan*

(Received 30 August 2002; revised manuscript received 7 March 2003; published 15 July 2003)

A comparative analysis of electron energy-loss spectroscopy (EELS) spectra for the 1D insulating cuprate Sr_2CuO_3 with transferred momentum $\vec{q} \parallel$ and $\perp$ to the chain axis allows one to elucidate the structure of the charge transfer gap in in-chain response. It is determined by the superposition of two types of excitations with different magnitudes of dispersion. The low-energy response with $\vec{q} \perp$ to the chain direction, but yet within the plane of CuO_4 plaquettes, exhibits also a dispersionless peak near 2 eV. The theoretical simulation of the EELS data using exact diagonalizations of an appropriate extended Hubbard Hamiltonian for relevant clusters requires the explicit consideration of low-lying oxygen $2p\pi$ states within the CuO_4 plaquette plane beyond the standard $pd\sigma$ extended Hubbard model widely used for cuprates with corner-shared CuO_4 plaquettes.

DOI: 10.1103/PhysRevLett.91.037001 PACS numbers: 74.72.Jt, 71.35.–y, 79.20.Uv

Low-energy ($\sim$ 2 to 3 eV) electron-hole (el-h) excitations in cuprates studied by electron energy-loss spectroscopy (EELS) provide insight into the involved orbitals. This knowledge is important for a proper description of these compounds in the framework of multiband Hubbard models. In particular, excitation spectra are of interest since they involve states which may affect also ground state properties of doped cuprates. Huge nonlinear optical (NLO) effects observed recently in Sr_2CuO_3 point to promising optoelectronic applications [1–4]. A thorough understanding of these nonlinearities demands a detailed knowledge of the excitation spectrum. El-h excitations in cuprates as pronounced charge transfer (CT) insulators are also interesting from a basic point of view, since they might considerably differ from excitons in standard Mott-Hubbard systems, conjugated polymers, molecular crystals, as well as in conventional band insulators [5].

To describe earlier EELS data of $Sr_2CuO_2Cl_2$ [5] Zhang and Ng (ZN) [6] proposed a model of CT excitons (CTE). The ZN-CTE is thought of as the CT of a hole with b_{1g} symmetry from one CuO_4 plaquette to a neighbor one forming a Zhang-Rice (ZR) singlet state there [5,6]. To explain also dispersionless, low-energy features in refined EELS data of this 2D cuprate, the ZN model was generalized in Ref. [7], where it was argued that a process generates one- and two-center excitons (OCE, TCE). Therefore the el-h pair is localized predominantly on one or two CuO_4 plaquettes, respectively (see Fig. 1). On the basis of this modified model incorporating all Cu $3d$ and O $2p$ orbitals the energies of a large number of CTE were predicted and a preliminary assignment of main features in the EELS spectra was achieved in a wide (2 ÷ 13 eV) energy range. However, in such 2D cuprates with spectra being a hardly resolved superposition of both types of CTE there remains still some ambiguity concerning the reliable assignment of two OCE and seven TCE.

Before discussing our results, we shortly overview the simple OCE model (see also Ref. [7]). With respect to symmetry aspects and the orbitals involved, the

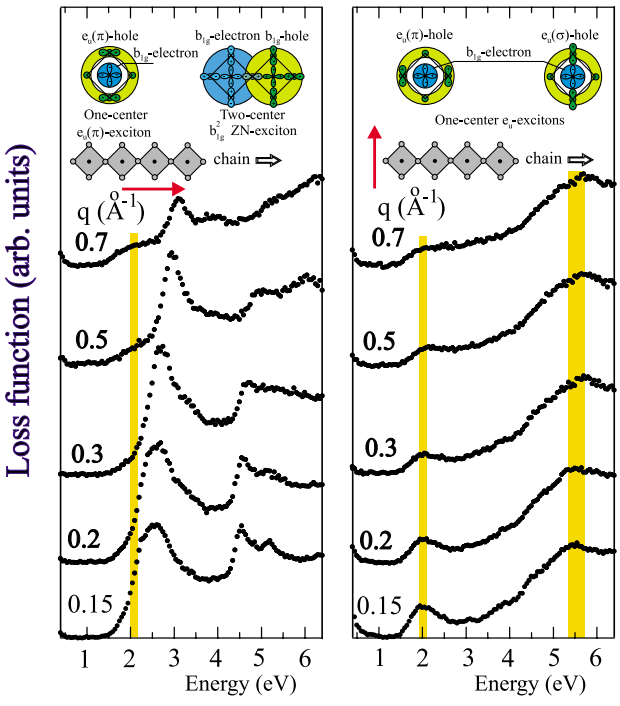

FIG. 1 (color online). EELS spectra in Sr_2CuO_3 for longitudinal ($\vec{q} \parallel \vec{a}$, left panel) and transversal ($\vec{q} \parallel \vec{b}$, right panel) responses with an illustration of one- and two-center excitons.

one-particle one-plaquette model provides a first step to estimate the dispersionless excitations. With 5 Cu $3d$ and 12 O $2p$ atomic orbitals for an idealized CuO_4 plaquette with D_{4h} symmetry [8], 17 symmetrized a_{1g}, a_{2g}, b_{1g}, b_{2g}, e_g and a_{2u}, b_{2u}, $e_u(\sigma)$, $e_u(\pi)$ orbitals can be formed. σ orbitals and π orbitals exhibit orientations of the O $2p$ lobes $\parallel$ and $\perp$ to a Cu-O bond, respectively. The even Cu $3d$ $a_{1g}(d_{z^2})$, $b_{1g}(d_{x^2-y^2})$, $b_{2g}(d_{xy})$, $e_g(d_{xz}, d_{yz})$ orbitals strongly hybridize with even combinations of O $2p$ orbitals of the same symmetry yielding bonding γ^b and antibonding γ^a states. Similarly, the purely O nonbonding orbitals $e_u(\sigma)$ and $e_u(\pi)$ hybridize with each other. Among numerous one-center el-h CT excitations the first candidates for dipole-active CTE within the plaquette plane are transitions from the b_{1g}^b ground state to purely O doublet $2p_\pi$-$2p_\sigma$ hybrid states $e_u^{a,b}$. The e_u^b and e_u^a states show a different O hole distribution. The former (latter) has predominantly O $2p_\pi$ ($2p_\sigma$) character. We denote these two states by their dominating character, π and σ, respectively, where π hereafter denotes π-oxygen orbitals lying within the plaquette plane. Thus, we expect two dipole-allowed OCE: the $e_u(\pi)$ and $e_u(\sigma)$ CTE. Their energies and the intensity ratio I_π/I_σ are affected by the p_π-p_σ mixing. For typical values of parameters we estimate

$$I_\pi/I_\sigma \approx |(t_{\sigma\sigma} + t_{\pi\pi})/(\Delta_{\sigma\pi})|^2 \leq 0.1, \qquad (1)$$

where $t_{\sigma\sigma}$, $t_{\pi\pi}$ are O transfer integrals, for σ and π bonds, respectively, and $\Delta_{\sigma\pi} = \epsilon_\sigma - \epsilon_\pi$, with ϵ_σ and ϵ_π being typical site energies for O $2p_\sigma$ and $2p_\pi$ states, respectively. Thus, the high-energy $e_u(\sigma)$ exciton is expected to show significant intensity both in optical and EELS spectra. Recent estimates [10–12] supporting angle resolved photoemission spectroscopy (ARPES) data [13,14] point to rather low-lying O $2p\pi$ states in corner-shared 1D and 2D cuprates with $\Delta_{\sigma\pi} \approx 1 \div 3$ eV [15].

Below we show that the response direction dependent EELS study of the 1D cuprate Sr_2CuO_3 with corner-shared CuO_4 plaquettes provides a rare opportunity to separate various types of CT excitations [16]. EELS probes the energy and momentum dependent loss function $P = \mathrm{Im}[-1/\epsilon(\omega, \vec{q})]$. Within the long-wavelength limit ($q \to 0$) the EELS selection rules are the same as in optics, if we choose $\vec{q} \parallel$ to the electric field $\vec{\mathcal{E}}$. However, in contrast to EELS, standard optical measurements (e.g., absorption) cannot distinguish nearly dispersionless from dispersive excitations. We argue that along with the in-chain response a 1D cuprate like Sr_2CuO_3 should reveal sizable low-energy "transversal" response for $\vec{\mathcal{E}}$ within the plane of CuO_4 plaquettes but $\perp$ to the chain axis $\vec{a}$. For this aim we have performed high-resolution EELS measurements also for this transversal case. Chain cuprates are good candidates for such a study since the scattering of electrons with a transferred momentum $\vec{q} \perp \vec{a}$ excites mainly el-h pairs on one CuO_4 plaquette.

In contrast, for $\vec{q} \parallel$ to the chain axis both types of excitons, OCE and TCE, are expected. The EELS spectra in "longitudinal" response have already been published and analyzed within standard one-, two-, and four-band extended Hubbard models [17–19]. However, such models can describe properly at most the in-chain optical response. Here we have included the in-chain EELS data, too, to provide the reader with a check of our seven-band model in both response cases. Incorporating *two* orbitals, $2p_\sigma$ and $2p_\pi$, at each O site, we arrive at our seven-band model [10] which generalizes the four-band picture. A similar six-band model for 2D cuprates has been proposed and mapped onto an effective one-band model in Ref. [20] to explain low-energy optical absorption and Raman data. Besides our orbitals their basis includes also Cu $3d_{xy}$ orbitals.

The EELS spectra for Sr_2CuO_3 for both response directions are shown in Fig. 1. They have been taken using thin films that have been cut using an ultramicrotome equipped with a diamond knife. For the transmission measurements the films have been mounted on standard microscopy grids (for details of the single crystalline sample preparation as well as a description of the measurement, see Ref. [17]). As expected, the two sets of spectra look rather different. In the transversal response, we observed well-defined EELS peaks at 2 and 5.5 eV. The intensity ratio [see Eq. (1)] and the lacking energy dispersion allow us to associate them with dipole-allowed CT transitions having a particularly "localized" nature. Moreover, comparing both spectra, we see that despite the strong inequivalence of spectra in longitudinal and transversal responses of Sr_2CuO_3, a low-energy peak near 2 eV is present in both responses. Though for in-chain response it is partly hidden for low q values by the intensive band peaked at 2.6 eV and seen as a shoulder, near π/a it is a well-separated weak peak due to the large blueshift of the intense neighbor. This might imply that the excitation is almost confined to a single CuO_4 plaquette, the only common element of $\parallel$ - and $\perp$ -scattering geometries in a 1D cuprate with corner-shared CuO_4 plaquettes. Hence, by keeping in mind the intensity ratio as well as our theoretical results shown in Fig. 2 we assign the peaks at 2 and 5.5 eV in the EELS spectrum with the OCE $e_u(\pi)$ and $e_u(\sigma)$, respectively.

To make our picture more quantitative and convincing, we have performed theoretical calculations of $P(\vec{q}, \omega)$ for Sr_2CuO_3 with the aid of the exact diagonalization technique. The linear-chain cuprate under consideration is modeled by finite Cu_nO_{3n+1} ($n = 2, \ldots, 4$) open chain clusters formed by n corner-shared CuO_4 plaquettes (see Fig. 1). We adopted the above mentioned seven-band extended Hubbard model. Along with standard $pd\sigma$ Hamiltonian parameters (here and below given in eV) $U_d = 9$, $U_p = 6$, $\Delta_{p\sigma d} = 3$, $t_{p\sigma d} = 1.3$ (in-chain direction), $\Delta_{\sigma\sigma} = 0.3$ (side and chain O difference), $t_{p\sigma d} = 1.4$ (side O), and $t_{\sigma\sigma} = 0.7$, as well as with the intersite

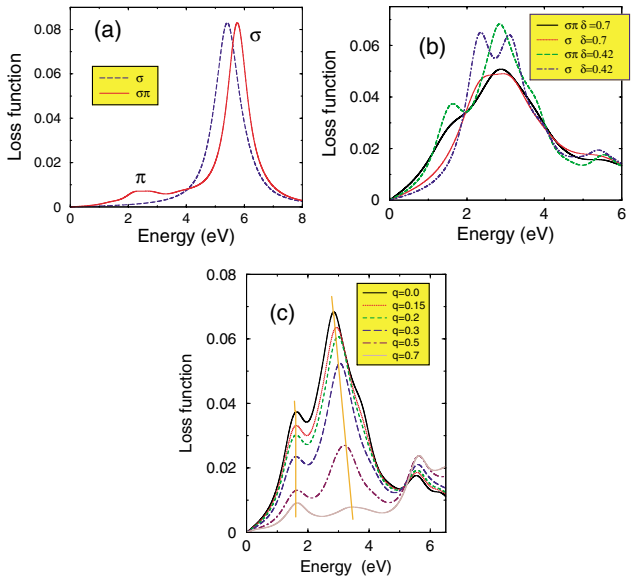

FIG. 2 (color online). Simulated EELS spectra. Transversal response for $\vec{q} = 0$ (a). Solid line: seven-band ($\sigma\pi$) model with low- (O $2p\pi$) and high-energy (O $2p\sigma$) excitations; dotted curve: four-band (σ) model without O $2p\pi$ states. In-chain response (b),(c) $\vec{q} = 0$ and various Lorentzian peak broadenings (at half width) δ in eV (b); $\vec{q} \neq 0$, $|\, q \,|$ in Å^{-1} as in Fig. 1 in reverse sequence from top to bottom (c). The nearly vertical curves connecting the maxima are guides to the eye to show the dispersion.

exchange interactions $K_{pd} = 0.2$, $K_{\sigma\sigma} = 0.02$ included, we made use of reasonable values for the parameters related to O π states: $t_{\pi\pi} = 0.6$, $t_{\sigma\pi} = 0.3$, and $\Delta_{p_y d} = 0.1$ (chain O), $\Delta_{p_x d} = 0.2$ (side O). In this notation the above mentioned $\Delta_{\sigma\pi}$ [see Eq. (1)] reads $\Delta_{\sigma\pi} = \Delta_{p\sigma d} - \Delta_{px,yd}$. For the additional Coulomb interactions we adopted $V_{\sigma\pi} = 3.8$ (on site), $V_{\sigma\pi} = 0.3$ (intersite), $V_{\pi\pi} = 0.5$, $V_{pd} = 0.9$ (1.0) for the Cu-O bond $\parallel$ ($\perp$) to the chain axis, respectively [10]. Finally, the remaining exchange parameters were taken as $K_{\sigma\pi} = 1.2$ (on site) and 0.01 (intersite).

We start with the canonical one-particle gap

$$E_g = E_G(+e) + E_G(-e) - 2E_G(0), \qquad (2)$$

where $E_G(0)$ and $E_G(\pm e)$ denote the ground state energy of the neutral chain and of the chain with one added (removed) electron e, respectively. Physically, it corresponds to the formation energy of an *independent* el-h pair at variance with a classical exciton with el-h Coulomb interaction included. With the parameter set mentioned above we arrive for a linear Cu_4O_{13} cluster at $E_g = 1.58$ eV. Next, the real part of the optical conductivity σ and the imaginary part of the dielectric function ε_2 related as $\sigma_1(\omega, q) = \omega\varepsilon_2(\omega, q)/4\pi$ have been calculated using standard Lanczos and continued fraction techniques [21]. Finally, one easily finds the real part ε_1 and the loss function $P = \varepsilon_2/(\varepsilon_1^2 + \varepsilon_2^2)$. In calculating P, a phenomenological isotropic background dielectric constant $\varepsilon_\infty = 5.8$ has been used in ε_1. Then we arrive at a slightly anisotropic static dielectric tensor: $\varepsilon_1(0) = 7.99$ and 6.4 in $\vec{a}$ (chain) and in $\perp$ ($\vec{b}$) directions, respectively, in accord with experimental data [17]. The calculated $P(\omega)$ are shown in Figs. 2(a)–2(c).

Turning to Fig. 2(a), we note that only the seven-band model with low-lying oxygen $2p\pi$ states within the plaquette plane enables us to reproduce the main features of the spectra in transversal response. The inspection of the hole occupation numbers in the low-energy excited states, which mainly contribute to the 2 eV peak in $P(\omega)$, reveals that there is a hole CT from the σ subsystem to the Oπ states, while for the transitions forming the peak near 5.5 eV an intra-σ subsystem CT is clearly dominant. The inspection of the spectra in the in-chain response shown in Figs. 2(b) and 2(c) reveals a negligible ≈ 0.1 eV (sizable $\sim$0.6 eV) dispersion of the first (second) peak, respectively, similarly to what is shown in Fig. 1. Both peaks contain *significant* O $2p\pi$ contributions. As expected, finite size effects are stronger (but already small at $n = 3, 4$) in the in-chain ($\perp$) response, respectively. Further refinement of our simulated spectra (e.g., with respect to the shoulder near 2 eV in the in-chain response which depends on details of the peak broadening [see Fig. 2(b)], a more detailed study of Hamiltonian parameters, as well as the analysis of charge-charge correlators which measure the internal exciton localization will be considered elsewhere. Finally, we note that p doping for our parameter set results in a non-neglible hole occupation of π orbitals even in the ground state at variance with the undoped case. This interesting fact might be related to small polaron transport features reported for p doped Sr_2CuO_3 [22,23].

In conclusion, EELS data for Sr_2CuO_3 in two response directions reveal the two-peak nature of the CT gap with the presence of nearly degenerate two types of excitations in the in-chain response. The first peak (shoulder) represents the optical counterpart of the so-called "1 eV peak" revealed by ARPES measurements in a number of cuprates and is roughly associated with the h-CT transition $b_{1g} \rightarrow e_u(\pi)$ from the Cu $3d$-O $2p$ hybrid state of b_{1g} symmetry to purely oxygen O $2p_\pi$ states almost localized on one CuO_4 plaquette, while the latter corresponds to the $b_{1g} \rightarrow b_{1g}$ CT transition between neighboring plaquettes with a ZR singlet as the final local 2h state [24]. Our experimental findings are supported by cluster model calculations with the inclusion of O $2p_\pi$ orbitals. To the best of our knowledge this is the first unambiguous manifestation for the relevance of O $2p_\pi$ holes for the low-energy excitations in a cuprate. The structure of the optical gap with two types of charge excitations seems to be generic for many parent cuprates which implies a revisit of some widely accepted views on their electron structure. The sizable dispersion of the most intense

low-lying CTE (in EELS at 2.6 eV) agrees with its two-center nature [5,6] that is fairly well confirmed in the studies of the NLO effects mentioned above [25]. In this context, we emphasize the decisive role of *direct* EELS measurements in the observation and assignment of two kinds of excitations in Sr_2CuO_3 as compared with conventional *indirect* optical data based on reflectivity measurements followed by a Kramers-Kronig transformation and accompanied by unavoidable uncertainties [26] regarding positions and intensities of weak spectral features. The loss function from EELS data is a powerful tool to examine subtle details of the energy spectrum and the dynamics of el-h excitations.

We thank J. Hirsch, P. Horsch, H. Eschrig, R. Kuzian, and H. Rosner for encouraging discussions. Support from grants by SMWK, DFG/SPP 1073 Fi-439/10-1 Es-85/8-1, and UAS No. 436 UKR 113/490, INTAS No. 01-0654, CRDF No. REC-005, RME No. E00-3.4-280 and No. UR.01.01.042, RFBR No. 01-02-96404 is gratefully acknowledged.

*Present address: R. Bosch GmbH, D-72703 Reutlingen, Germany.
†Electronic address: drechsler@ifw-dresden.de

[1] T. Ogasawara *et al.*, Phys. Rev. Lett. **85**, 2204 (2000).
[2] H. Kishida *et al.*, Nature (London) **405**, 929 (2000).
[3] T. Manako *et al.*, Appl. Phys. Lett. **79**, 1754 (2001).
[4] M. Ashida *et al.*, Appl. Phys. Lett. **78**, 2831 (2001).
[5] Y. Y. Wang *et al.*, Phys. Rev. Lett. **77**, 1809 (1996).
[6] F. C. Zhang and K. K. Ng, Phys. Rev. B **58**, 13520 (1998).
[7] A. S. Moskvin *et al.*, Phys. Rev. B **65**, 180512(R) (2002).
[8] Strictly speaking, all 1D cuprates have CuO_4 plaquettes with D_{2h} symmetry, only, and one should distinguish between OCE involving "side-" from those with "in-chain" O sites. Two different O sites have been observed in O 1*s* x-ray absorption spectra [9]. There are also slightly different Cu-O bond lengths and transfer integrals [10].
[9] R. Neudert *et al.*, Phys. Rev. B **62**, 10 752 (2000).
[10] S.-L. Drechsler *et al.*, J. Low Temp. Phys. **117**, 407 (1999).
[11] L. F. Mattheiss *et al.*, Phys. Rev. B **40**, 2217 (1989).
[12] R. Hayn *et al.*, Phys. Rev. B **60**, 645 (1999).
[13] J. J. M. Pothuizen *et al.*, Phys. Rev. Lett. **78**, 717 (1997).
[14] C. Dürr *et al.*, Phys. Rev. B **63**, 014505 (2000).
[15] Nonbonding O states manifest themselves also in ARPES which, in contrast with optics and EELS, probes one-particle excitations. At the Γ point the same selection rules hold for ARPES, optical, and EELS transitions. ARPES "sees" only the purely O e_u photoholes, or, strictly speaking, the ^1E_u states of the two-hole CuO_4^{5-} center with a $b_{1g}e_u$-like configuration. The inspection of the ARPES spectra [13,14] for $Sr_2CuO_2Cl_2$ gives valuable information on two low-lying ^1E_u states. It reveals two strong bands separated from the ground state ZR singlet by $1.5 \div 2$ eV and ≈ 5 eV, which could be ascribed to the low-energy $e_u(\pi)$ and high-energy $e_u(\sigma)$ photohole states, respectively. More correctly, one should speak about $b_{1g}^b e_u(\pi)$ and $b_{1g}^b e_u(\sigma)$ configurations.
[16] In principle, similar information can be gained using inelastic x-ray scattering. It has been recently applied to study the in-chain response of Sr_2CuO_3 by M. Z. Hasan *et al.*, Phys. Rev. Lett. **88**, 177403 (2002). There, a slightly higher dispersion of charge excitations ≈ 1 eV has been found (compare with ≈ 0.7 eV in our EELS data). Probably due to the smaller resolution the O $2p\pi$ related nondispersive shoulder seen in EELS near 2.2 eV (see Fig. 1) could not be resolved.
[17] R. Neudert *et al.*, Phys. Rev. Lett. **81**, 657 (1998).
[18] K. Penc and W. Stephan, Phys. Rev. B **62**, 12 707 (2000).
[19] A. Hübsch *et al.*, Phys. Rev. B **63**, 205103 (2001).
[20] M. E. Simón *et al.*, Phys. Rev. B **54**, R3780 (1996).
[21] E. Dagotto, Rev. Mod. Phys. **66**, 763 (1994).
[22] W. B. Archibald *et al.*, Phys. Rev. B **52**, 16 101 (1995).
[23] Y. J. Shin *et al.*, Z. Anorg. Allg. Chem. **616**, 201 (1992).
[24] The cluster model predicts another TCE $b_{1g}e_u(dp\pi)$ at 1–2 eV above the $b_{1g}^2(pd)$ one (see Ref. [7]) which is seen within in-chain response near 4.5 eV.
[25] Indeed, our analysis of the photoinduced absorption and the third-order NL susceptibility $\chi^{(3)}$ in Sr_2CuO_3 [1,2] allows one to reveal the near degeneracy of both even (S) and odd (P) types of TCE, which can be subdivided into S and P excitons with an energy of ~ 2 eV. The estimate of the transition matrix element $d = |\langle S|\hat{\mathbf{d}}|P\rangle| \approx 2eR_{\mathrm{CuCu}} \approx 2e \times 4$ Å (see Fig. 4 in Ref. [2]) points to a TCE, since it probes its effective "size." In addition, the NLO response of Sr_2CuO_3 [2] reveals a weak feature redshifted ~ 0.3 eV with respect to the main TCE. It can be ascribed to a weak OCE that seems yet to be overlooked in available reflectivity data of Sr_2CuO_3 [26]. The large dipole moment d between excited S and P excitons estimated above is important in explaining the NLO effects.
[26] M. Imada *et al.*, Rev. Mod. Phys. **70**, 1039 (1998). Thin film absorption in $\perp$ response [3] shows a peak near 3.2 eV at variance with these data and EELS. Anyhow, it cannot be described within the usual $pd\sigma$ model, too.